PNAS RESEARCH ARTICLE | ECOLOGY OPEN ACCESS

Long-term benefits of nonpharmaceutical interventions for endemic infections are shaped by respiratory pathogen dynamics

Rachel E. Baker[a,b,1], Chadi M. Saad-Roy[c,d,e], Sang Woo Park[b], Jeremy Farrar[f], C. Jessica E. Metcalf[b,g], and Bryan T. Grenfell[b,g]

Edited by Ron Brookmeyer, Johns Hopkins School of Public Health, Baltimore, MD; received May 23, 2022; accepted October 31, 2022 by Editorial Board Member Kenneth W. Wachter

COVID-19 nonpharmaceutical interventions (NPIs), including mask wearing, have proved highly effective at reducing the transmission of endemic infections. A key public health question is whether NPIs could continue to be implemented long term to reduce the ongoing burden from endemic pathogens. Here, we use epidemiological models to explore the impact of long-term NPIs on the dynamics of endemic infections. We find that the introduction of NPIs leads to a strong initial reduction in incidence, but this effect is transient: As susceptibility increases, epidemics return while NPIs are in place. For low R_0 infections, these return epidemics are of reduced equilibrium incidence and epidemic peak size. For high R_0 infections, return epidemics are of similar magnitude to pre-NPI outbreaks. Our results underline that managing ongoing susceptible buildup, e.g., with vaccination, remains an important long-term goal.

SARS-CoV-2 | masking | dynamics

Significance

Nonpharmaceutical interventions, such as mask wearing, introduced to limit the spread of COVID-19 have proved effective at reducing cases of other respiratory diseases. A key public health question is whether these interventions could be introduced long term to limit outbreaks of diseases such as influenza. Here, we use epidemic models to show that the effect of mask wearing on endemic disease is likely short lived. Over longer time horizons, outbreaks may return while interventions are in place, as population immunity decreases.

Nonpharmaceutical interventions (NPIs), including mask wearing and social distancing, have proved crucial for reducing the transmission of SARS-CoV-2 prior to the development and deployment of vaccines. At the same time, these interventions have also limited the transmission of other respiratory pathogens including respiratory syncytial virus (RSV) and influenza (1). During winter 2020 in the southern hemisphere, and winter 2020/2021 in the northern hemisphere, cases of respiratory infections fell dramatically compared to previous seasons (2–4). The US Centers for Disease Control (CDC) reported 2,857 total positive influenza specimens for the 2020/2021 season from combined clinical and public health labs when compared to 229,551 positive specimens in the 2018/2019 season (5). In Australia, 598 cases of influenza were confirmed in 2021 compared to 313,000 in 2019 (6).

Given the observed efficacy of NPIs for reducing the incidence of influenza and RSV, a key public health question is whether interventions should continue to be implemented long term to reduce future burden from endemic disease (7). Mask wearing has been shown to be highly effective at reducing the transmission of respiratory, airborne pathogens in laboratory studies (8, 9). Moreover, in some countries, the practice of wearing masks precedes the emergence of COVID-19. A study conducted in Japan in 2012 found that 38% of survey respondents wore a mask during the 2011/2012 influenza season (10). Mask wearing, prior to COVID-19, was also common in China, Taiwan, and Hong Kong, with the practice gaining popularity during and following the SARS-CoV pandemic in 2003 (11, 12). Yet, the long-run effectiveness of mask wearing for reducing the transmission of endemic diseases, as opposed to emerging pathogens such as SARS-CoV and SARS-CoV-2, remains unclear. Notably, a crude comparison of influenza attack rates between Japan (13) and the USA (14) reveals broadly similar values (see also Fig. 4).

Here, we use epidemiological models to explore the impact of possible long-run NPIs, including mask wearing, on the dynamics of endemic, acute directly-transmitted infections. We focus on the transmissibility of the pathogen which is captured by the basic reproduction number, R_0, as well as the duration of immunity to the disease. NPIs enter the model by lowering the transmission rate, β, which biologically reflects per-pair transmission; we assume that NPIs do not impact the recovery rate following infection. We first consider the implications for two types of pathogen: a low R_0 pathogen with waning immunity, i.e., "influenza-like," and a high R_0 pathogen with longer-lasting immunity, i.e, "RSV-like." For the low R_0 pathogen we assume susceptible-infected-recovered-susceptible (SIRS) dynamics where the return to susceptibility reflects the pathogen evolving to evade host immunity or waning immunity. For the high R_0 pathogen, we assume susceptible-infected-recovered (SIR) dynamics. In this case, increases in the susceptible population are driven by births. These two models have seasonal transmission rates:

Author affiliations: [a]Department of Epidemiology, Brown School of Public Health, Providence, RI 02903; [b]Department of Ecology and Evolutionary Biology, Princeton University, Princeton, NJ 08544; [c]Lewis-Sigler Institute for Integrative Genomics, Princeton University, Princeton, NJ 08540; [d]Miller Institute for Basic Research in Science, University of California, Berkeley, CA 94720; [e]Department of Integrative Biology, University of California, Berkeley, CA 94720; [f]Wellcome Trust, London NW1 2BE, UK; and [g]School of Public and International Affairs, Princeton University, Princeton, NJ 08540

Author contributions: R.E.B., C.M.S.-R., and B.T.G. designed research and performed research; R.E.B., C.M.S.-R., and S.W.P. analyzed data; R.E.B., C.M.S.-R., S.W.P., J.F., C.J.E.M., and B.T.G. wrote the paper.

The authors declare no competing interest.

This article is a PNAS Direct Submission. R.B. is a guest editor invited by the Editorial Board.

[1]To whom correspondence may be addressed. Email: rebaker@brown.edu.

This article contains supporting information online at http://www.pnas.org/lookup/suppl/doi:10.1073/pnas.2208895119/-/DCSupplemental.

Published November 29, 2022.

in the influenza model, seasonal transmission is driven by the seasonality of specific humidity in New York (15), and in the RSV model, the transmission rate is derived by fitting the model to data from Texas (1). Following this analysis, we derive the analytical solution using a more generic form of the SIR and SIRS models with varied R_0 and immunity length.

Results

Fig. 1*A* shows the model results for the influenza-like pathogen. The model assumes that mean R_0 prior to the implementation of NPIs is approximately 1.8 and the duration of immunity is 40 wk and the duration of infectiousness is 1 wk. The NPIs are included as a fixed 20% reduction in transmission for 1 y, starting in 2020, followed by a year without NPIs to reflect the implementation and then reduction of COVID-19 controls. Early estimates suggest that transmission of respiratory pathogens declined by at least 20% in the United States at the start of the pandemic (1, 16–18) (results for different percentage reductions are shown in *SI Appendix*, Fig. 2). As NPI measures are relaxed, the model predicts an out-of-season resurgence in cases driven by an increase in the susceptible population during the NPI period, as described in previous work (1). To explore the impact of long-term NPIs on future outbreaks, we introduce a second NPI period as a 20% reduction in transmission that lasts indefinitely (i.e., reflecting possible ongoing mask wearing). The secondary NPIs lead to an immediate decline in case numbers. However, after 1 to 2 y, modeled incidence resurges even while NPIs remain in place. Crucially, the proportion of susceptible individuals rises over the NPI period and stabilizes at a new mean, at which point, seasonal epidemics return albeit at a reduced epidemic peak size.

We repeat the exercise in Fig. 1*B* for RSV, a pathogen with higher R_0 (19). We use a model fit to data from Texas where we estimate mean $R_0 = 7$ and the birth rate is the 2020 birth rate in Texas. Again, we assume an initial 20% reduction in transmission, followed by a year without NPIs, and then reintroduce the NPIs permanently at a 20% reduction in transmission. During the initial NPI period, modeled RSV cases decline substantially but resurge when NPIs are removed (1). During the secondary NPI period, modeled RSV outbreaks return after 3 to 4 y of low case numbers. However, on returning, RSV resumes a seasonal pattern of outbreaks that are strikingly similar to the pre-NPI era in terms of timing and magnitude. This result contrasts with the low R_0 SIRS model where outbreaks during the NPI period remain of reduced peak size. Population-level susceptibility to RSV increases substantially over the secondary NPI period (blue line Fig. 1*A*), eventually settling on a higher mean susceptible proportion. We find a similar result even with more stringent controls, though epidemics take longer to reestablish (*SI Appendix*, Fig. 2).

To interpret this result, we calculate a moving average of the effective reproduction number (R_e, which is equal to R_0 multiplied by the proportion susceptible S/N) over the modeled period (gold line, Fig. 1*A*). During the first and early second phases of NPIs R_e declines below pre-NPI levels. Later, during the second phase of NPIs, higher susceptibility drives up R_e such that after 3 to 4 y, R_e returns to pre-NPI equilibrium levels. Collectively, these results imply that control measures such as mask wearing are effective at reducing the incidence of endemic disease in the short-term, as evinced by the observed reduction in RSV and influenza cases during the COVID-19 pandemic (1, 2). However, over the long term, substantial reductions in incidence are hard to maintain, particularly for high R_0 pathogens. These effects derive from the dynamics of susceptibility; long-term NPIs may lead to a substantial increase in susceptibility that can lead to a spike in incidence if later relaxed or if a more transmissible strain emerges (*SI Appendix*, Fig. 2).

Our model results reveal a distinct difference in the behavior of a low R_0 pathogen (influenza) and high R_0 pathogen RSV during a period of ongoing NPIs. Whilst NPIs are in place, epidemics of both pathogens return; yet, the low R_0 epidemics are reduced in epidemic peak size while the high R_0 epidemics appear unaffected. To explore this result in the general case, we turn to a simple unforced SIR model with demography (Fig. 2*A*). We simulate the dynamics of an infection where $R_0 = 8$, the birth rate is set equal to the mortality rate, the duration of infectiousness is 2 wk, and a 20% reduction in transmission (β) occurs during the NPI period. In the time series (*Top Left*, Fig. 2*A*) and S–I phase plane plot (*Right side*, Fig. 2*A*), we recover our results from Fig. 1*B* wherein the proportion infected returns to similar levels during the NPI period. The S–I phase plane plot reveals that NPIs shift the epidemic to a different attractor defined by higher equilibrium susceptibility.

We can capture the impact of NPIs across infections of different R_0, for example, influenza and RSV, via equilibrium analysis (20). Beginning with the fully immunizing, unforced

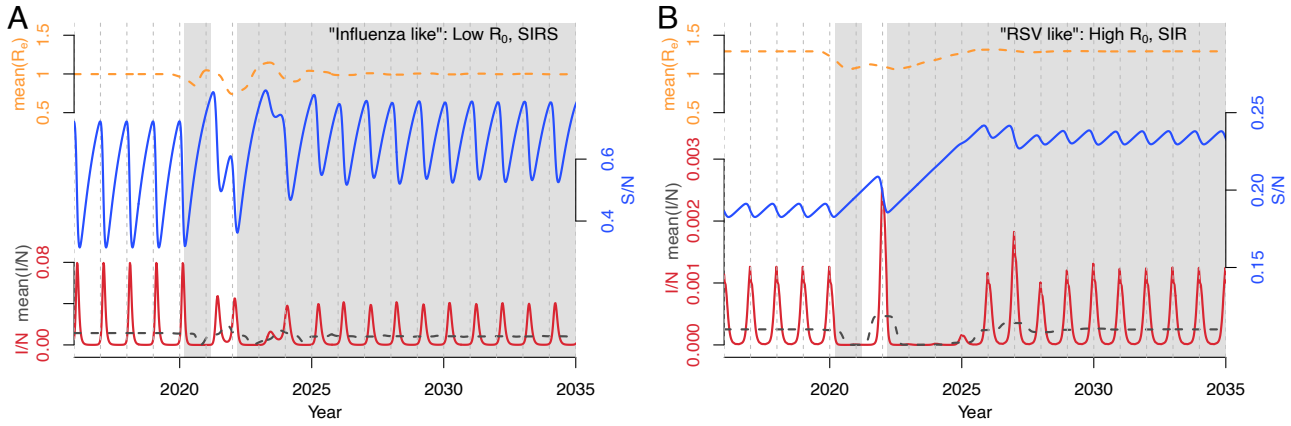

Fig. 1. Epidemics return while controls are in place. Impact of NPIs on proportion infected (I/N, red line), 52-wk rolling average of proportion infected (mean I/N, black dashed line), proportion susceptible (S/N, blue line), and 52-wk rolling average of the effective reproduction number (mean R_e, gold line) shown for two phases (gray shaded time period) of 20% reduction in transmission for influenza (*A*) and RSV (*B*). Recruitment of susceptibles is primarily driven by waning immunity for (*A*) and births in (*B*).

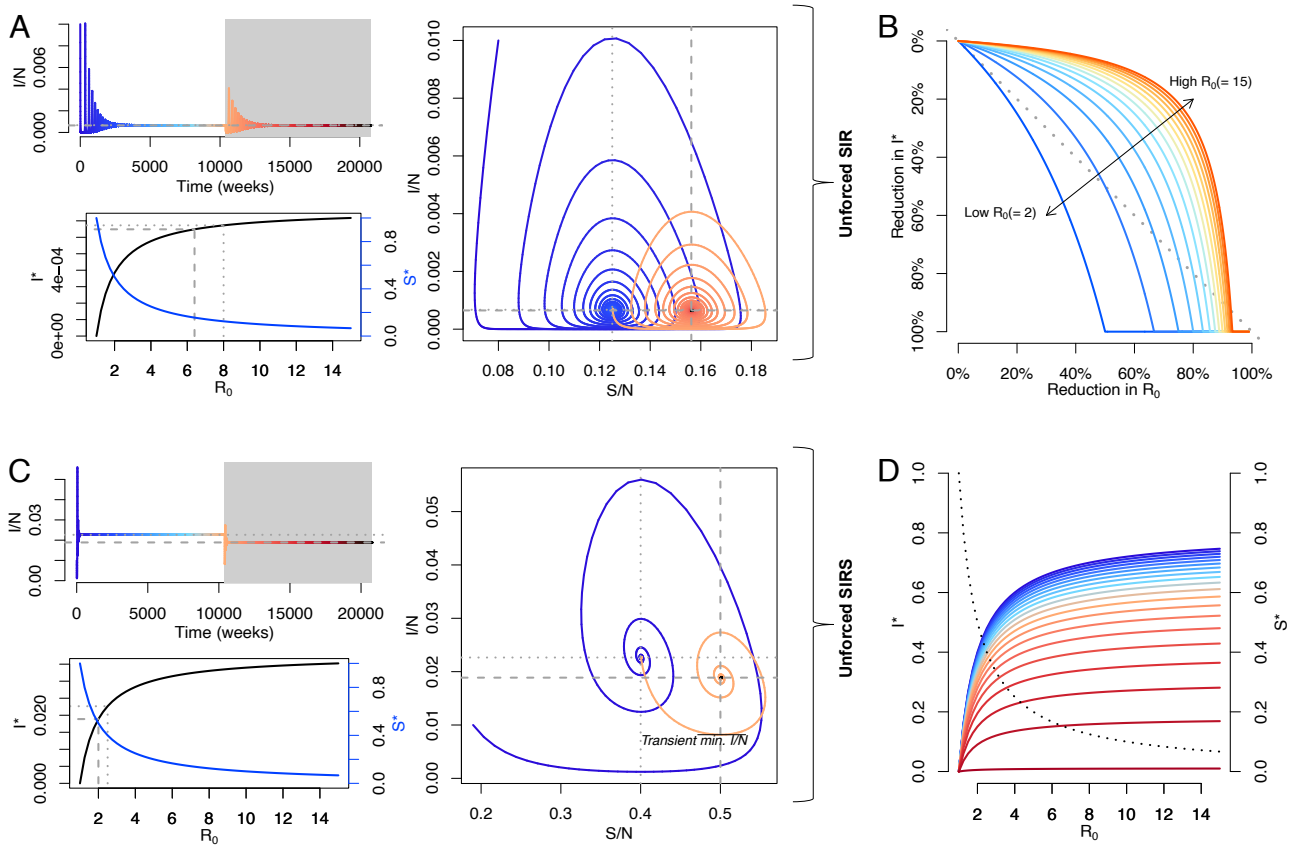

Fig. 2. Analytical results using unforced SIR/SIRS models (*A*) Time series (*Top Left*), S–I phase plane (*Right*), and equilibrium solution (*Lower Left*) for the unforced SIR model with demography. Gray shading in time series plot represents the implementation of a 20% reduction in transmission. Dotted lines represent equilibrium proportion infected and susceptible (I^* and S^*) for a pathogen with $R_0 = 8$, and dashed lines represent I^* and S^* following a 20% reduction in transmission. (*B*) Shows percentage reduction in I^* against R_0 for pathogens with R_0 increasing from 2 to 15 by 1 (color gradient). (*C*) Shows the same plots as (*A*), but for an SIRS pathogen model where the duration of immunity is 52 wk. Dotted lines and time series plot now represent a pathogen with $R_0 = 2.5$ and dashed lines a 20% reduction in transmission. (*D*) Shows the dependence of I^* (colored lines) on the duration of immunity varied from 0.5 (blue) to 200 (red) wk. Dashed lines represent the relationship between R_0 and S^* which is insensitive to the duration of immunity.

SIR model, we examine the analytical solution for the equilibrium proportion infected I^* and proportion susceptible S^* and plot these as a function of R_0 in *Lower Left* Fig. 2*A* (for derivation see *Materials and Methods*). I^* has a nonlinear relationship with R_0 and is a linear transformation of $-1/R_0$ (Fig. 2*A*). Pathogens with a high R_0 sit on the flat part of the I^* curve such that reductions in R_0 due to NPIs do not substantially impact the proportion infected. In contrast, for a pathogen with a lower R_0 (e.g., 1–4), a reduction in R_0 due to NPIs will yield a greater percentage reduction in equilibrium cases. We show this explicitly in Fig. 2*B*, where the dashed $y = -x$ line corresponds to a scenario where the NPI-driven percentage reduction in transmission exactly equals the percentage reduction in equilibrium infected. For an SIR pathogen with $R_0 = 2$, a 10% reduction in transmission leads to an 11% reduction in I^*. However, for a pathogen with $R_0 = 3$, a 10% reduction in transmission leads to a 6% reduction in I^*. For higher transmission pathogens, reducing R_0 has minimal impact on I^* unless substantial reductions are made.

We find similar results for the unforced SIRS model (Fig. 2*C*). In this model, susceptibility is driven by waning immunity (where the duration of immunity is equal to 1 y) as well as births (set equal to the mortality rate). In the time series and S–I phase plane plot (*Top Left* and *Right side* of Fig. 2*C*), we simulate a pathogen with $R_0 = 2.5$ and a 20% reduction in transmission during the NPI period. For this lower R_0 pathogen, reducing transmission leads to a clearer reduction in I^* (as shown by comparing the time series in Fig. 2*B* to Fig. 2*A*). However, the equilibrium I^* still remains substantially above the transient, short-term reductions in incidence observed when the NPI measures are initially put into place (Fig. 2*C* S–I phase plane plot). For SIRS infections in general, I^* remains a linear transformation of $-1/R_0$ (*Lower Left*, Fig. 2*C*). In Fig. 2*D*, we vary the duration of immunity in the SIRS model. Notably, equilibrium S^* remains unchanged, given by $S^* = 1/R_0$, while I^* declines as the duration of immunity increases. The SIS model, where the duration of immunity is zero, gives qualitatively similar conclusions (*Materials and Methods*).

The analytical solution to the SIR and SIRS models shows that for high R_0 infections, such as RSV, the equilibrium impact of NPIs may be more limited in terms of reducing infections in the medium-to-longer term. For low R_0 infections, such as seasonal influenza, NPIs may drive stronger effects. Crucially for both pathogen types, short-term reductions in incidence may substantially exceed the long-term, equilibrium effect. This suggests that the clear and important reduction in cases of endemic, respiratory pathogens during the COVID-19 pandemic may not persist long term and hence does not reflect the true efficacy of NPIs at controlling endemic infections in the long run. Importantly, the qualitative results do not hinge on the values of the duration of infectiousness, duration of immunity, or birth/mortality rates (*SI Appendix*, Figs. S3 and S4).

While the efficacy of long-term NPIs may be limited for certain pathogens, a combined approach that employs vaccines as well as

NPIs may be highly effective at reducing infections. In Fig. 3A, we take the RSV model from Fig. 1*B* and assume that NPIs are implemented for 3 y that reduce transmission by 20%. After 3 y, a vaccine is introduced that is administered to infants at birth that reduces infection and has 80% coverage (applying a vaccination rate across the whole population generates a similar picture; see *SI Appendix*, Fig. 7). Following vaccine introduction, mean proportion infected remains permanently lowered and NPIs successfully minimize outbreaks prior to vaccine introduction (see *SI Appendix*, Fig. 6 for comparison case). In Fig. 3*B*, we show the analytical result for the impact of a vaccination that reduces infection and NPIs on I^* . Increasing vaccination coverage has a linear effect on reducing I^*. NPIs may further reduce I^* by lowering R_0 and increasing the probability of local elimination. It is important to note that the vaccines we consider here reduce infection. The introduction of a vaccine that reduced severe disease but not infection would not impact I^*. In contrast, if a vaccine were introduced that reduced transmission it would mirror the effect of the NPIs.

In certain countries, mask wearing has been a common practice prior to the COVID-19 pandemic. Our results imply that for a low-R_0 pathogen such as influenza, NPI measures including mask wearing could have a modest effect on influenza case numbers. An international comparison of influenza attack rates is difficult due to differences in reporting and surveillance across countries. Improved availability of serological data may enable these comparisons in the future (21). Instead, we look at the implications of mask wearing for epidemic intensity, a measure of how concentrated cases are through the year. More intense outbreaks, i.e., a higher number of cases within a fixed period, can represent a larger burden to healthcare systems depending on available resources. Crucially, the intensity of the outbreaks can be compared across regions despite differences in reporting and surveillance. Our measure of epidemic intensity is equal to 0 if cases are exactly evenly distributed throughout the year and 1 if cases are concentrated in one week of the year (*Materials and Methods*) (22).

We first consider changes in epidemic intensity for a simple SIRS model with seasonal forcing assuming a 20% reduction in transmission (Fig. 4*A*). Following the introduction of NPIs, intensity declines and cases become more spread out through the year. In Fig. 4*B*, we show the dependence of both intensity and mean proportion infected on the reduction in R_0 (where mean R_0 is 1.8). We find similar declines in both intensity and mean proportion infected as more stringent NPIs are introduced. In Fig. 4*C*, we plot intensity against latitude for all countries reporting data to the World Health Organization's Global Influenza Programme as well as data from Hong Kong. Latitude is a key determinant of epidemic intensity, with less intense outbreaks occurring close to the tropics likely driven by climatic factors (15, 23). We highlight in blue locations where mask wearing is more frequently practiced and sample red locations where mask wearing is not practiced. On average, locations with seasonal mask wearing have a slightly reduced epidemic intensity compared to predicted levels based on latitude alone. However, while latitude is a significant predictor of outbreak intensity ($P \ll 0.001$), mask wearing was not found to be significant ($P = 0.10$). Importantly, many other factors including contact patterns and birth rates could drive cross country differences in outbreak intensity.

Discussion

There are several caveats to our analysis. First, the long-term impact of NPIs depends on the basic reproduction number of the pathogen, however, values of R_0 are typically hard to determine and likely vary by location. For example, we estimate a mean R_0 of 7 for RSV in Texas, while other studies in the United States estimate an R_0 between 8.9 and 9.2 (16, 19). Studies that assume a full return to susceptibility following RSV infection tend to report lower R_0 estimates, i.e., $R_0 \approx 2$, however, this assumption does not appear realistic based on serological evidence (24). Second, we have not explicitly addressed how NPI measures may impact the age distribution of infections. In the classical unforced SIR model, the mean age of infection is inversely proportional to R_0 (20), suggesting that NPIs will have relatively modest effects on the mean age of infection for high R_0 pathogens. However, even small changes could make a big difference if vulnerability and transmission changes quickly with age. We explore age-structure using a simple model with two age classes (*SI Appendix*, Figs. S8 and S9 and *Supporting Methods*). Age heterogeneity of NPIs is important but does not qualitatively

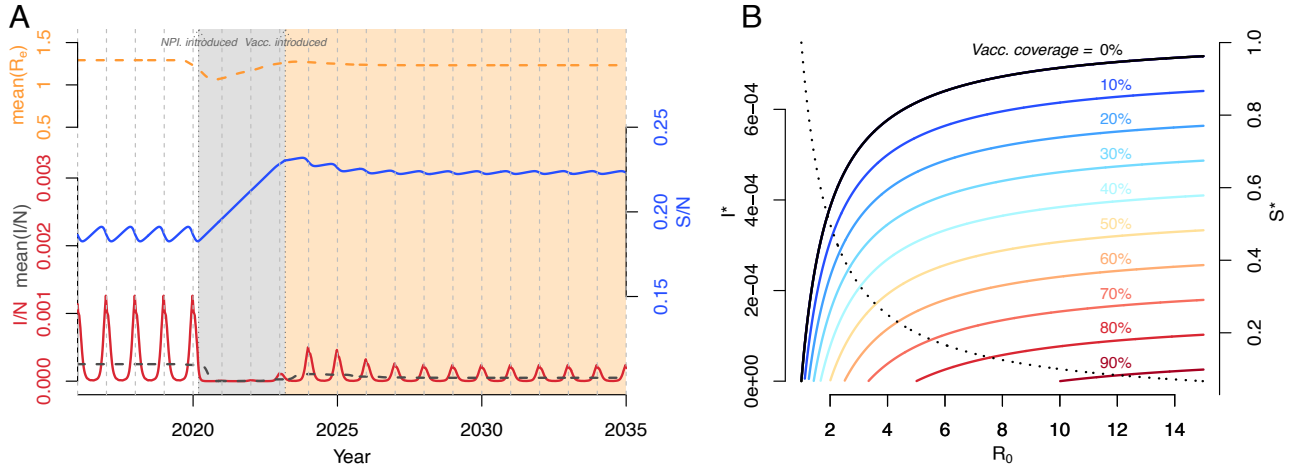

Fig. 3. Combined control measures. (*A*) Line colors are the same as Fig. 1*A*. The shaded gray region represents a 20% reduction in transmission due to NPIs, and the shaded orange region represents the introduction of vaccines at birth with 80% coverage, while NPIs remain in place. (*B*) Shows the analytical solution to the SIR model with demography and flexible vaccine coverage from zero coverage (black line) to 90% coverage (red line). S^* is shown with the dashed black line.

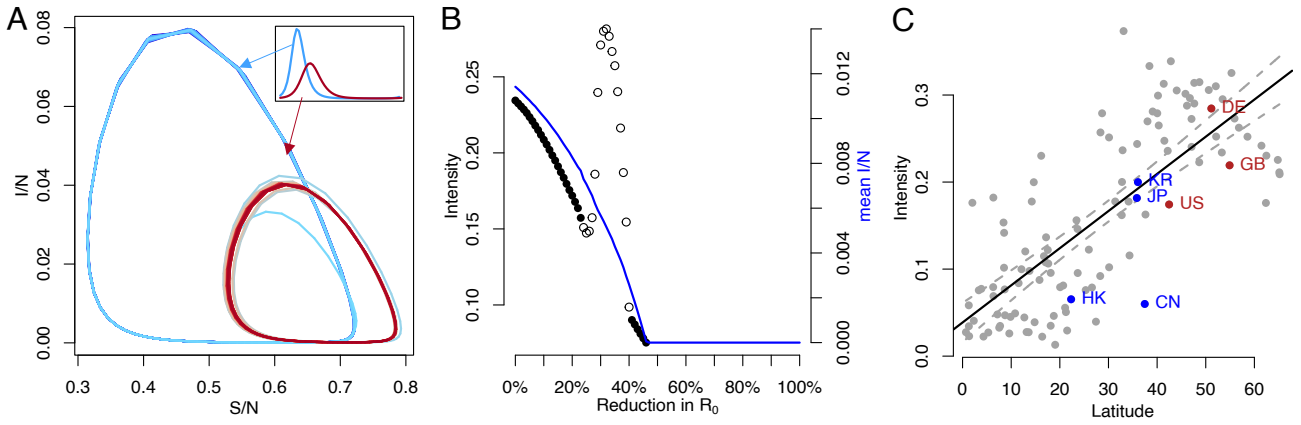

Fig. 4. NPI impact on epidemic intensity. (*A*) S–I phase plane showing a 20% reduction in transmission on a seasonally forced SIRS model with mean $R_0 = 1.8$. Inset time series shows the proportion infected over one year pre (blue) and post (red) NPIs. (*B*) Shows epidemic intensity (black points for annual epidemics and hollow points for biennial epidemics) and mean proportion infected (blue line) for reductions in R_0 where $R_0 = 1.8$. (*C*) Shows estimated influenza epidemic intensity against latitude for 113 countries and Hong Kong. Solid line and dashed line show the regression of latitude on intensity and the 95% CI, respectively. Blue points are countries with pre-COVID-19 mask wearing. Red points are example countries without pre-COVID-19 mask wearing.

impact results. A more comprehensive age-structured model that captures the dynamics of multiple age classes should be explored in future work. Finally, we have not considered the evolutionary consequences of implementing long-term NPIs, particularly for influenza. Evidence from the COVID-19 NPI period suggests prolonged low circulation has reduced the diversity of influenza viruses and perhaps resulted in the extinction of the B/Yamagata lineage (25). Given that such periods of very low circulation are likely temporary, it is unclear how influenza evolution may be affected by NPIs in the long term (26).

Broadly our results underline the importance of NPIs in limiting major outbreaks (*SI Appendix*, Fig. S2). Indeed, sufficiently effective implementation of NPIs can eliminate transmission [e.g., the elimination of enteric infections by water treatment and sewerage (27)]. Below this elimination threshold, we find that the long-term impact of NPIs on endemic infections depends on the dynamics of population susceptibility. After implementation of NPIs, cases may decline, but over time, population susceptibility increases driving up the effective reproduction number R_e and increasing the likelihood of a return epidemic. When such an outbreak occurs, population susceptibility stabilizes at a new equilibrium level where the mean proportion infected may be similar in size to the pre-NPI levels albeit dependent on the basic reproduction number of the pathogen. This result has implications for both the long-term control of endemic infections as well as understanding the circulation of endemic infections over the coming years, as COVID-19 NPIs continue to be implemented in response to SARS-CoV-2 variants. In the latter case, our results imply that endemic infections such as RSV and influenza may return even if COVID-19 NPIs are ongoing.

The most powerful use case of NPI measures for endemic infections is in combination with vaccination. Vaccines are highly effective at reducing infections; NPIs can provide a temporary control during or preceding vaccine distribution. Importantly, a combination of NPIs and vaccination could move endemic infections closer to the elimination threshold, especially for infections with intrinsically lower R_0. Simple models also underline that vaccination is relatively robust to reductions in uptake (e.g., due to vaccine hesitancy). Since vaccination does not cause a rise in susceptibility (20) (*SI Appendix*, Figs. S6 and S7), a sharp reduction in uptake does not lead to an immediate large outbreak; by contrast, a sharp drop in NPI adoption could lead to a rapid epidemic due to the previous buildup of susceptibles (*SI Appendix* Fig. S6). A combination of susceptible limitation by vaccination and NPIs is thus particularly powerful. Advances in vaccine development brought about by the global COVID-19 response should be leveraged to control the full range of endemic pathogens.

Materials and Methods

RSV and Influenza Models. RSV and influenza models are shown in Fig. 1. The time series susceptible-infected-recovered (TSIR) model for RSV is fully described in previous work (1). The model (shown in Fig. 1 and *SI Appendix*, Fig. S2) is parameterized using RSV hospitalization data from Texas. Model simulations are run for weekly time steps according to

$$I_t = \frac{\beta_{t-1} I_{t-1}^{\alpha} S_{t-1}}{N_{t-1}} c, \quad [1]$$

$$S_t = S_{t-1} + B_{t-1} - I_t, \quad [2]$$

where I_t and S_t are number of infected and susceptible individuals at time t, N_t is the population size, B_t is the weekly birth rate, and β_t is the seasonal transmission rate estimated biweekly for 52 wk (*SI Appendix*, Fig. S1). α is a constant that captures heterogeneities in mixing and the discretization of a continuous time process, fixed at 0.97 based on previous work (1, 28). Simulations are run for 50 y to remove transient dynamics. NPIs are characterized as a percentage reduction in β for a fixed time period, i.e., a 20% reduction is β means 0.8*β. The reduction in beta approximates a 20% reduction in per-pair transmission. Further details of TSIR model fitting are provided in the *SI Appendix, Supporting Methods*.

The influenza model is SIRS where transmission is dependent on specific humidity, as described in previous work (15, 29, 30). The model equations are the following:

$$\frac{dS}{dt} = \frac{R}{L} - \frac{\beta(t) I S}{N} + \mu(N - S), \quad [3]$$

$$\frac{dI}{dt} = \frac{\beta(t) I S}{N} - \frac{I}{D} - \mu I, \quad [4]$$

$$\frac{dR}{dt} = \frac{I}{D} - \frac{R}{L} - \mu R, \quad [5]$$

where S is the proportion susceptible, I is the proportion infected, R is the proportion recovered, and N is the total population (where $S + I + R = N = 1$).

L is the duration of immunity, set at 40 wk. Waning immunity reflects the evolution of the pathogen to evade host immunity leading to reinfection. D is the duration of infectiousness, set at 1 wk. The model includes a weekly birth rate μ, equal to the mortality rate μ, set at 0.00038 or 1/(50*52). Transmission β is related to the basic reproduction number $R_0(t) = \beta(t)D$ which is dependent on specific humidity according to

$$R_0(t) = \exp(-180 * q(t) + \log(R_{0max} - R_{0min})) + R_{0min}, \quad [6]$$

where q_t is humidity and $R_{0max} = 3$ and $R_{0min} = 1.2$. We use a sinusoidal function for humidity that is derived from average New York humidity data. The functional form of the relationship between specific humidity is based on prior work by Shaman et al. (15, 29). When NPIs enter the model (Fig. 1*A*), they act to reduce $R_0(t)$ such that a 20% reduction is $R_0(t) * 0.8$.

Generalized SIR and SIRS Models. The generalized SIR and SIRS models are shown in Fig. 2. The generalized SIRS model is described by

$$\frac{dS}{dt} = \mu(N - S) - \frac{\beta IS}{N} + \omega R, \quad [7]$$

$$\frac{dI}{dt} = \frac{\beta IS}{N} - (\mu + \gamma)I, \quad [8]$$

$$\frac{dR}{dt} = \gamma I - \mu R - \omega R, \quad [9]$$

where μ is the birth rate, γ is the recovery rate, and ω is the rate at which immunity wanes. S, I, and R are defined as above. Setting the duration of immunity $\omega = 0$ recovers our generalized form of the SIR model. We derive the endemic equilibrium by setting $\frac{dI}{dt} = 0$ (31). Setting $N = 1$, from Eq. **8** we find

$$I(\beta S - (\gamma + \mu)) = 0, \quad [10]$$

where the disease free equilibrium is recovered when $I^* = 0$. The endemic equilibrium is when $S^* = \frac{\gamma+\mu}{\beta}$ or:

$$S^* = \frac{1}{R_0}. \quad [11]$$

Note that the equation for S^* is independent of ω and therefore the equilibrium proportion susceptible is the same for both SIR and SIRS model described here. By substituting **11** into Eq. (**7**), we find the equilibrium proportion infected:

$$I^* = \frac{\mu(R_0 - 1) + \omega(R_0 - 1)}{\beta + \omega R_0} = \frac{\mu + \omega}{\mu + \omega + \gamma}\left(1 - \frac{1}{R_0}\right). \quad [12]$$

for the SIRS model. For the SIR model, $\omega = 0$, and the equilibrium proportion infected is the following:

$$I^* = \frac{\mu(R_0 - 1)}{\beta} = \frac{\mu}{\mu + \gamma}\left(1 - \frac{1}{R_0}\right). \quad [13]$$

For the simulations in Fig. 2, we set $\gamma = 1/2$, $\mu = 1/(50 * 52)$, and $\omega = 1/52$ for the SIRS model. For the SIR model, $R_0 = 8$ and for the SIRS model, $R_0 = 2.5$.

SIS model. The generic susceptible-infected-susceptible model is the following:

$$\frac{dS}{dt} = \mu(N - S) - \frac{\beta IS}{N} + \gamma I, \quad [14]$$

$$\frac{dI}{dt} = \frac{\beta IS}{N} - (\mu + \gamma)I. \quad [15]$$

Again, the equilibrium proportion susceptible is given by $S^* = 1/R_0$. The equilibrium proportion infected can be found either by substituting S^* in equation (14) or from noting that $(N = S^* + I^*)$ such that if $N = 1$, $I^* = 1 - 1/R_0$.

Vaccination.

Vaccination at birth. Fig. 3 considers vaccination at birth. Vaccination at birth enters the generalized SIR model via the susceptible equation as

$$\frac{dS}{dt} = \mu(N(1 - p) - S) - \frac{\beta IS}{N}, \quad [16]$$

where p is the proportion of the birth cohort that are vaccinated. The equations for the infected population and the recovered population are given by Eqs. **8** and **9** with $\omega = 0$. Using Eq. **8** and assuming $N = 1$, we find again that the equilibrium proportion susceptible is $S^* = 1/R_0$. The equilibrium proportion infected is given by

$$I^* = \frac{\mu}{\mu + \gamma}\left((1 - p) - \frac{1}{R_0}\right), \quad [17]$$

i.e., I^* is again a linear transformation of $1/R_0$.

Vaccination at rate, total population. Vaccination may also occur at the population level. We consider vaccination at a rate v in the SIR model. The susceptible and infected equations are given as follows:

$$\frac{dS}{dt} = \mu(N(1 - p) - S) - \frac{\beta IS}{N} - vS, \quad [18]$$

$$\frac{dI}{dt} = \frac{\beta IS}{N} - (\mu + \gamma + v)I. \quad [19]$$

Setting $\frac{dI}{dt} = 0$ and rearranging Eq. **19**, we find $S^* = \frac{\mu+\gamma+v}{\beta}$. Given that $\gamma \gg v$ and μ, $S^* \approx 1/R_0$. Note that is infected individuals are unable to seroconvert, the vaccination term is removed from Eq. **19**, and $S^* = 1/R_0$.

Nullclines for both the vaccination at birth and vaccination at rate models are shown in *SI Appendix*, Fig. S7.

Epidemic Intensity. We define the epidemic intensity based on Dalziel et al. (22) as

$$Intensity = 1 - \frac{\sum p \ln(p)}{\ln(1/52)}, \quad [20]$$

where p is a vector of the mean number of influenza cases per week divided by the sum across all weeks. The mean number of cases per week is calculated by averaging across all years using weekly influenza country-level time series from 2012–2019. The denominator in Eq. **16** normalizes the intensity metric such that $Intensity = 0$, when cases are exactly evenly distributed across all 52 wk of the year. For years where there are 53 wk, the 53rd wk is removed.

Data, Materials, and Software Availability. Code data have been deposited in Github (https://github.com/rebaker/longterm_NPI).

ACKNOWLEDGMENTS. CMSR acknowledges the support from the Natural Sciences and Engineering Research Council of Canada through a Postgraduate-Doctoral Scholarship and from a Charlotte Elizabeth Procter Fellowship of Princeton University, and a Miller Research Fellowship from the Miller Institute for Basic Research in Science of UC Berkeley.

1. R. E. Baker *et al.*, The impact of Covid-19 nonpharmaceutical interventions on the future dynamics of endemic infections. *Proc. Natl. Acad. Sci. U.S.A.* **117**, 30547–30553 (2020).
2. J. van Summeren *et al.*, Low levels of respiratory syncytial virus activity in Europe during the 2020/21 season: What can we expect in the coming summer and autumn/winter? *Eurosurveillance* **26**, 2100639 (2021).
3. S. G. Sullivan *et al.*, Where has all the influenza gone? The impact of Covid-19 on the circulation of influenza and other respiratory viruses, Australia, March to September 2020. *Eurosurveillance* **25**, 2001847 (2020).
4. J. W. Tang *et al.*, Where have all the viruses gone? Disappearance of seasonal respiratory viruses during the Covid-19 pandemic. *J. Med. Virol.* **93**, 4099 (2021).
5. Centers for Disease Control and Prevention, Weekly U.S. influenza surveillance report. https://www.cdc.gov/flu/weekly/index.htm. Accessed 1 March 2022.
6. "Australia influenza surveillance report" (Australian Government Department of Health Tech. Rep. No. 1, 2022)
7. C. Pagel, "Back to normal" isn't enough. *Science* **375**, 1069 (2022).

8. J. Pan, C. Harb, W. Leng, L. C. Marr, Inward and outward effectiveness of cloth masks, a surgical mask, and a face shield. *Aerosol. Sci. Tech.* **55**, 718–733 (2021).
9. J. Howard, et al., An evidence review of face masks against Covid-19. *Proc. Natl. Acad. Sci. U.S.A.* **118** (2021).
10. K. Wada, K. Oka-Ezoe, D. R. Smith, Wearing face masks in public during the influenza season may reflect other positive hygiene practices in Japan. *BMC Public Health* **12**, 1–6 (2012).
11. J. T. Lau, S. Griffiths, K. C. Choi, C. Lin, Prevalence of preventive behaviors and associated factors during early phase of the H1N1 influenza epidemic. *Am. J. Infect. Control* **38**, 374–380 (2010).
12. B. J. Cowling, Y. Zhou, D. Ip, G. Leung, A. E. Aiello, Face masks to prevent transmission of influenza virus: A systematic review. *Epidemiol. Infect.* **138**, 449–456 (2010).
13. K. Taniguchi *et al*., Epidemiology and burden of illness of seasonal influenza among the elderly in Japan: A systematic literature review and vaccine effectiveness meta-analysis. *Influenza Other Respir. Virus.* **15**, 293–314 (2021).
14. J. I. Tokars, S. J. Olsen, C. Reed, Seasonal incidence of symptomatic influenza in the United States. *Clin. Infect. Dis.* **66**, 1511–1518 (2018).
15. J. Shaman, V. E. Pitzer, C. Viboud, B. T. Grenfell, M. Lipsitch, Absolute humidity and the seasonal onset of influenza in the continental United States. *PLoS Biol.* **8**, (2010).
16. Z. Zheng, V. E. Pitzer, E. D. Shapiro, L. J. Bont, D. M. Weinberger, Re-emergence of respiratory syncytial virus following the Covid-19 pandemic in the United States: A modeling study. medRxiv (2021).
17. Y. Qi, J. Shaman, S. Pei, Quantifying the impact of Covid-19 nonpharmaceutical interventions on influenza transmission in the United States. *J. Infect. Dis.* **224**, 1500–1508 (2021).
18. R. E. Baker, W. Yang, G. A. Vecchi, C. J. E. Metcalf, B. T. Grenfell, Assessing the influence of climate on wintertime SARS-CoV-2 outbreaks. *Nat. Commun.* **12**, 1–7 (2021).
19. V. E. Pitzer *et al*., Environmental drivers of the spatiotemporal dynamics of respiratory syncytial virus in the United States. *PLoS Pathogens* **11**, e1004591 (2015).
20. R. M. Anderson, R. M. May, *Infectious Diseases of Humans: Dynamics and Control* (Oxford University Press, 1992).
21. M. J. Mina *et al*., Science forum: A global immunological observatory to meet a time of pandemics. *Elife* **9**, e58989 (2020).
22. B. D. Dalziel *et al*., Urbanization and humidity shape the intensity of influenza epidemics in US cities. *Science* **362**, 75–79 (2018).
23. C. Viboud, W. J. Alonso, L. Simonsen, Influenza in tropical regions. *PLoS Med.* **3** (2006).
24. F. W. Henderson, A. M. Collier, W. A. Clyde Jr, F. W. Denny, Respiratory-syncytial-virus infections, reinfections and immunity: A prospective, longitudinal study in young children. *N. Engl. J. Med.* **300**, 530–534 (1979).
25. M. Koutsakos, A. K. Wheatley, K. Laurie, S. J. Kent, S. Rockman, Influenza lineage extinction during the Covid-19 pandemic?. *Nat. Rev. Microbiol.* **19**, 741–742 (2021).
26. B. T. Grenfell *et al*., Unifying the epidemiological and evolutionary dynamics of pathogens. *Science* **303**, 327–332 (2004).
27. V. E. Pitzer *et al*., Predicting the impact of vaccination on the transmission dynamics of typhoid in South Asia: A mathematical modeling study. *PLoS Negl. Trop. Dis.* **8**, e2642 (2014).
28. R. E. Baker *et al*., Epidemic dynamics of respiratory syncytial virus in current and future climates. *Nat. Commun.* **10**, 1–8 (2019).
29. J. Shaman, M. Kohn, Absolute humidity modulates influenza survival, transmission, and seasonality. *Proc. Natl. Acad. Sci. U.S.A.* **106**, 3243–3248 (2009).
30. W. Yang, M. Lipsitch, J. Shaman, Inference of seasonal and pandemic influenza transmission dynamics. *Proc. Natl. Acad. Sci. U.S.A.* **112**, 2723–2728 (2015).
31. M. J. Keeling, P. Rohani, *Modeling Infectious Diseases in Humans and Animals* (Princeton University Press, 2011).